eISSN (Online): 2598-0580

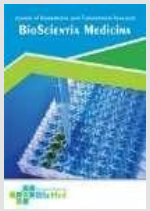

Bioscientia Medicina: Journal of Biomedicine & Translational Research

Journal Homepage: www.bioscmed.com

Periosteal Stripping Induces Comparable Early Callus Formation but Late-Phase Regression: A Histomorphometric and Machine-Learning Analysis in a Rat Femoral Fracture Model

Chandra Budi Hartono[1*], Udi Herunefi Hancoro[2], Ida Bagus Budhi Surya Adnyana[3]

[1]Department of Surgery, Faculty of Medicine, Universitas Sebelas Maret/Dr. Moewardi Regional General Hospital, Surakarta, Indonesia

[2]Department of Orthopedic Surgery, Faculty of Medicine, Universitas Sebelas Maret/Dr. Moewardi Regional General Hospital, Surakarta, Indonesia

[3]Department of Digestive Surgery, Faculty of Medicine, Universitas Sebelas Maret/Dr. Moewardi Regional General Hospital, Surakarta, Indonesia

ARTICLE INFO

Keywords:
Fracture healing
Histomorphometry
Machine learning
Periosteum
TRAP staining

***Corresponding author:**
Chandra Budi Hartono

E-mail address:
chandrabudih13@gmail.com

All authors have reviewed and approved the final version of the manuscript.

https://doi.org/10.37275/bsm.v10i4.1567

A B S T R A C T

Background: The periosteum is critical for fracture healing, serving as a reservoir for osteoprogenitor cells and vascular supply. A clinical paradox exists where periosteal stripping is considered detrimental yet is historically associated with hypertrophic overgrowth. This study investigates the temporal paradox of periosteal stripping, testing the hypothesis that it induces a biphasic response characterized by early inflammatory compensation followed by late-phase regenerative failure. **Methods:** Twenty-four male Sprague-Dawley rats were randomized into four groups (n=6/group): Intact Periosteum (PI) and Periosteal Stripping (PS), evaluated at 14 and 28 days post-fracture. Mid-diaphyseal femoral fractures were stabilized with 1.0 mm K-wires. Healing was quantified using a validated Modified Allen-Huo Histological Score (0-10) and Trainable Weka Segmentation (TWS) for tissue classification. Osteoclast activity was assessed via Tartrate-Resistant Acid Phosphatase (TRAP) staining. **Results:** At Day 14, the PS group exhibited healing comparable to the PI group (Median Score: 8.0 [IQR 8.0–9.0] vs. 8.0 [IQR 7.0–8.0]; $p = 0.176$), driven by hypertrophic soft callus formation rather than true osteogenesis. However, by Day 28, the PS group demonstrated significant regression (Median Score: 3.5 [IQR 3.0–4.8]) compared to the PI group (Median Score: 8.0 [IQR 8.0–8.0]; $p = 0.006$). Quantitative histomorphometry revealed significantly higher osteoclast density in the PS-28 group (TRAP+ cells: 18.5 ± 2.1/field) compared to PI-28 (4.2 ± 1.1/field; $p < 0.001$), indicating active resorption of the unstable callus. **Conclusion:** Periosteal stripping does not accelerate early healing but induces a volume-matched inflammatory callus that fails to consolidate. The significant late-phase regression underscores the vital role of the cambium layer in definitive remodeling. Surgical preservation of the periosteum is mandated to prevent atrophic non-union.

1. Introduction

The trajectory of modern trauma surgery is increasingly defined by a collision between technological advancement and the immutable biological constraints of tissue regeneration.[1] Among the myriad challenges facing the global orthopedic community, the burden of traumatic bone fractures has escalated into a critical public health emergency. Recent epidemiological data underscore a shifting landscape where musculoskeletal injuries are no longer merely transient events but chronic determinants of global health. According to the World

Health Organization and comprehensive analyses from the Global Burden of Disease studies, fractures account for a disproportionate and rising share of Disability-Adjusted Life Years (DALYs) worldwide.[2] The socioeconomic ramifications of this silent epidemic are staggering; in 2023 alone, the aggregated economic impact of fracture management, rehabilitation, and associated productivity losses was estimated to exceed 518 billion dollars globally. This financial hemorrhage is driven by a dual-demographic pincer movement: the escalating incidence of high-energy trauma from road traffic accidents in developing nations, and the exponential rise of fragility fractures within the rapidly aging populations of the developed world.

While the mechanical evolution of orthopedic fixation—from the early days of traction to the modern era of locking compression plates and intramedullary nails—has revolutionized the immediate stabilization of trauma, biological failure remains a persistent adversary. Despite optimal mechanical environments, the complication of non-union or delayed union continues to plague approximately 5 to 10 percent of all long bone fractures. These failures represent more than statistical outliers; they translate into prolonged morbidity, opioid dependence, profound psychological distress, and the necessity for repeated, often morbid, surgical interventions. Consequently, the frontier of fracture care has shifted from purely mechanical engineering to biological orchestration, necessitating a deeper understanding of the cellular and molecular determinants of repair.[3]

The biological success of fracture repair is conceptually governed by the diamond concept, a framework that mandates the simultaneous presence of four essential pillars: mechanical stability, adequate vascularity, osteogenic precursor cells, and an osteoconductive scaffold.[4] In the context of long bone healing, the physiological lynchpin of this system is the periosteum. This highly vascularized, specialized connective tissue membrane, which envelopes the cortical bone, is not merely a passive sheath but a dynamic biological organ. Structurally, the periosteum is biphasic, organized into an outer fibrous layer responsible for mechanical integrity and limiting extrusion, and an inner cambium layer. It is this inner layer that serves as the engine of regeneration, functioning as a rich reservoir of mesenchymal stem cells (MSCs), fibroblasts, and committed osteoprogenitor cells.[5]

The functional primacy of the periosteum is most evident during the immediate post-traumatic period. In the early phases of secondary fracture healing, the periosteum acts as the primary source of chondrocytes and osteoblasts that proliferate to form the soft callus.[6] This initial biological bridge is critical; it stabilizes the fracture gap and provides the cartilaginous template for endochondral ossification long before the medullary circulation, often disrupted by the injury, can be re-established. Furthermore, the periosteum contributes significantly to the cortical blood supply, delivering oxygen and nutrients essential for the metabolically demanding process of osteogenesis.

Despite the unequivocal biological importance of the periosteum, its management during surgical intervention remains the subject of a profound clinical paradox. The standard of care for Open Reduction and Internal Fixation (ORIF) inherently places the surgeon in a position of conflict with biology. To achieve anatomical reduction and apply rigid fixation devices such as plates and screws, the surgeon must perform periosteal stripping. This maneuver, while mechanically necessary to seat the implant directly against the bone, inflicts significant biological collateral damage. Stripping mechanically disrupts the vital cambium layer, effectively removing the local population of osteoprogenitor cells, and severs the periosteal arterioles, thereby devascularizing the outer third of the bone cortex.[7]

This leads to a controversial dichotomy in orthopedic literature. On one hand, the destruction of the periosteum is viewed as a detriment to healing, a necessary evil of surgery that predisposes the bone to atrophic non-union. On the other hand, historical clinical observations, particularly in pediatric

orthopedics, suggest a counter-narrative. In children, traumatic periosteal elevation often results in robust, sometimes excessive, localized overgrowth, implying that the trauma of separation may actually stimulate an osteogenic response. This contradiction raises a fundamental biological question: Does periosteal injury act as a purely destructive force, stripping the bone of its regenerative potential, or does it trigger a compensatory, albeit transient, inflammatory response that mimics accelerated healing in the short term?

To resolve this paradox, one must examine the molecular landscape of fracture repair. Healing is driven by a complex, temporally regulated symphony of signaling pathways.[8] The Wnt/beta-catenin pathway governs the differentiation of MSCs into osteoblasts, while the Bone Morphogenetic Protein (BMP) axis is essential for driving chondrogenesis and subsequent endochondral ossification. Periosteal stripping disrupts this orchestration in two distinct ways. First, it physically removes the cellular responders—the cambium cells—that would normally react to these signals. Second, and perhaps more deceptively, it induces a localized hypoxic environment. The disruption of periosteal blood flow stabilizes Hypoxia-Inducible Factor 1-alpha (HIF-1 alpha), which in turn upregulates the expression of vascular endothelial growth factor (VEGF).[9]

We hypothesize that this interplay creates a temporal paradox in healing kinetics. The acute trauma of stripping, combined with the release of pro-inflammatory cytokines (such as IL-1 and IL-6) and hypoxic stress, may trigger a massive recruitment of stem cells from the surrounding soft tissue envelope (the myoperiosteal niche). This could result in an initial, robust formation of inflammatory callus—an early gain. However, this extrinsic cellular response may be unsustainable. Without the intrinsic regenerative capacity of the definitive cambium layer to guide the transition from soft callus to hard callus, the healing process may stall, leading to a failure of consolidation and regression of bone quality—the late loss.

Validating this biphasic hypothesis requires a shift in methodological rigor. To date, few studies have quantified these temporal nuances with sufficient precision. The majority of historical research relies on traditional histomorphometry, which is often hampered by manual, subjective scoring systems. These semi-quantitative methods are prone to significant inter-observer variability and may fail to detect subtle microstructural changes in tissue composition. The evolution of computational biology offers a solution. The integration of machine learning algorithms, specifically Trainable Weka Segmentation (TWS) on the ImageJ platform, provides a novel approach to tissue analysis. By training algorithms to recognize specific texture and color features, researchers can now objectively quantify tissue classes—differentiating fibrous tissue, cartilage, woven bone, and lamellar bone—with pixel-level precision, removing human bias from the equation.[10]

This study aims to rigorously evaluate the longitudinal effect of periosteal stripping on fracture healing kinetics in a Sprague-Dawley rat model, utilizing high-precision histomorphometry. The novelty of this research is threefold: (1) The Temporal Paradox: It is the first to explicitly characterize the biphasic nature of periosteal trauma, identifying an early inflammatory acceleration that paradoxically leads to a late-phase regressive failure; (2) Machine Learning Validation: It employs advanced machine-learning-assisted segmentation (Trainable Weka Segmentation) to provide an objective, quantitative validation of traditional histological scoring; (3) Mechanistic Correlation: It provides a comprehensive mechanistic explanation for non-union by correlating late-stage healing failure with specific cellular activity, specifically the upregulation of osteoclast-mediated resorption as evidenced by Tartrate-Resistant Acid Phosphatase (TRAP) staining. By dissecting the timeline of early gain and late loss, this study seeks to resolve the clinical controversy surrounding periosteal management and provide biological evidence to support periosteal-sparing surgical techniques.

2. Methods

This study employed a randomized, controlled, experimental design using a Posttest-Only Control Group structure. The protocol was reviewed and approved by the Institutional Animal Care and Use Committee (IACUC) of the Faculty of Medicine, Universitas Sebelas Maret (Protocol ID: EC-2024-08-112). All procedures adhered to the ARRIVE guidelines (Animal Research: Reporting of In Vivo Experiments) and the 3Rs principle (Replacement, Reduction, Refinement).

Twenty-four male Sprague-Dawley rats (*Rattus norvegicus*), aged 10 to 12 weeks and weighing 250 to 300 grams, were selected. The Sprague-Dawley model was chosen due to its well-documented consistent fracture healing timeline, which closely parallels the stages of human secondary bone healing, albeit at an accelerated rate where 1 day in rats approximates 2 to 3 days in humans. An a priori power analysis was conducted using G*Power 3.1. Based on previous studies measuring histological healing scores (mean difference expected = 3.0, SD = 1.5), a sample size of n=6 per group was calculated to achieve a Power (1-beta) of 0.80 and an alpha error probability of 0.05. While n=6 is the minimum threshold for non-parametric analysis, it is consistent with ethical standards for pilot mechanistic studies in orthopedic research.

The animals were acclimatized for 7 days and then randomized into four groups using a computer-generated block randomization sequence: (1) PI-14 (Control): Intact Periosteum, euthanized at Day 14; (2) PS-14 (Experimental): Periosteal Stripping, euthanized at Day 14; (3) PI-28 (Control): Intact Periosteum, euthanized at Day 28; (4) PS-28 (Experimental): Periosteal Stripping, euthanized at Day 28. Surgery was performed under general anesthesia utilizing Ketamine (80 mg/kg) and Xylazine (10 mg/kg) intraperitoneally. The right hind limb was shaved and sterilized. A 2-cm lateral incision was made to expose the femur. The vastus lateralis was split bluntly to minimize soft tissue damage. In the periosteal intervention (PI) groups, the periosteum was preserved with utmost care. In the periosteal stripping (PS) groups, a circumferential strip of periosteum measuring exactly 5 mm in length was removed from the mid-diaphysis using a sharp micro-elevator and scalpel. This 5-mm defect exceeds the critical regenerative gap for the periosteum itself, ensuring no immediate sliding of the cambium layer over the fracture site. A transverse mid-diaphyseal osteotomy was created using a Gigli saw to prevent thermal necrosis. Retrograde fixation was achieved using a 1.0 mm Kirschner wire (K-wire) introduced into the medullary canal. K-wire fixation provides relative stability, allowing for micromotion at the fracture site. This setup was deliberately chosen to induce secondary fracture healing, characterized by callus formation, which is the standard biological response reliant on the periosteum, as opposed to primary healing seen with rigid plate fixation. The muscle and fascia were closed with 4-0 absorbable sutures, and the skin was closed with 4-0 nylon.

Femora were harvested, stripped of soft tissue while leaving the callus intact, and fixed in 10% neutral buffered formalin for 48 hours. Decalcification was performed using 10% EDTA (pH 7.4) for 4 weeks. Samples were dehydrated, embedded in paraffin, and sectioned at 5 μm thickness; (1) Hematoxylin & Eosin (H&E): For general cellular architecture and scoring; (2) Masson's Trichrome: To differentiate collagen fibers (blue) from osteoid (red); (3) Tartrate-Resistant Acid Phosphatase (TRAP): To identify active osteoclasts. Sections were incubated in TRAP staining solution (Sigma-Aldrich, Kit 387A) for 1 hour at 37°C. TRAP-positive multinucleated cells (defined as having 3 or more nuclei) located on the bone surface were counted.

To ensure reproducibility and address the subjectivity of histological analysis, we employed a dual-modality assessment. Two blinded pathologists independently scored the slides using a validated Modified Allen-Huo Scoring System (Table 1), which evaluates the fracture gap bridging and callus maturity.

Table 1. Modified Allen-Huo Histological Scoring System

Criteria used for semi-quantitative assessment of fracture healing and callus maturity.

SCORE	DESCRIPTION OF CALLUS MORPHOLOGY
0	**No Bridging:** Pure fibrous tissue or fluid remains in the fracture gap; no evidence of stabilization.
1 - 2	**Fibrous Union:** Predominantly fibrous tissue; cartilage presence is minimal (less than 25%). No bony continuity.
3 - 4	**Mixed Soft Callus:** A mixture of fibrous and cartilaginous tissue; initial appearance of woven bone islands (intramembranous ossification).
5 - 6	**Cartilaginous Bridging:** Predominantly cartilaginous bridging across the gap; woven bone formation exceeds 50% of the callus area.
7 - 8	**Complete Bony Bridging:** Fracture gap is fully bridged by woven bone; initial signs of cortical remodeling and hard callus consolidation.
9 - 10	**Definite Union & Remodeling:** Mature lamellar bone formation; recanalization of the marrow cavity; cortical continuity is fully restored.

Digitized slides were analyzed using ImageJ equipped with the Trainable Weka Segmentation (TWS) plugin. The Random Forest classifier was trained on a subset of 50 images using user-defined traces for four classes: Mineralized Bone, Cartilage/Osteoid, Fibrous Tissue, and Background/Marrow. The classifier achieved a Dice Coefficient of 0.88 and Pixel Accuracy of 92% against manual ground-truth segmentation, validating its utility for this dataset. The software quantified the percentage area of each tissue type and Total Callus Area (mm^2).

All statistical computations were executed using the Statistical Package for the Social Sciences (SPSS) software, version 26.0 (IBM Corp., Armonk, NY). Given the experimental design involving a small sample size (n=6 per group) and the semi-quantitative nature of the histological scoring system, the underlying assumption of normality was rigorously assessed prior to hypothesis testing. The Shapiro-Wilk test confirmed a non-normal distribution for the histological scores ($p < 0.05$), indicating a significant deviation from Gaussian principles. Consequently, parametric descriptors such as Mean and Standard Deviation were deemed inappropriate for this dataset. Instead, all descriptive data are presented as the Median with the corresponding Interquartile Range (IQR) to provide a robust measure of central tendency and dispersion that is resistant to the influence of outliers.

Inferential analysis employed non-parametric protocols to ensure statistical validity. To assess global differences across the four distinct experimental cohorts (PI-14, PS-14, PI-28, and PS-28), the Kruskal-Wallis H test was utilized as the non-parametric equivalent to the one-way analysis of variance (ANOVA). Following the detection of significant global variance, *post-hoc* pairwise comparisons were conducted using the Mann-Whitney U test. This method was specifically selected to evaluate differences between independent groups,

facilitating comparisons of treatment effects at specific time points, such as the comparison between PS-14 and PI-14, as well as temporal changes between distinct cohorts, such as the difference between PS-14 and PS-28. It is methodologically pertinent to note that the Wilcoxon Signed-Rank test was explicitly excluded; as the Day 14 and Day 28 groups comprised different animals sacrificed at their respective endpoints, the data represented independent rather than paired longitudinal samples. For all analyses, a two-tailed p-value of less than 0.05 was considered statistically significant.

3. Results

Table 2 delineates the divergent microstructural evolution of the fracture callus observed between the intact and stripped cohorts. In the early reparative phase (Day 14), the Intact Periosteum (PI) group exhibited a physiologically distinct healing architecture, characterized by a well-contained soft callus with chondrocytes arranged in organized columns, indicative of robust endochondral ossification. In sharp contrast, the Periosteal Stripping (PS) group, while quantitatively matching the control in callus volume, displayed a pathological morphology. The callus was voluminous and disorganized, composed primarily of hypertrophic cartilage and fibrous tissue that invaded the surrounding musculature, a phenomenon morphologically consistent with a myositis ossificans-like reaction.

By the late remodeling phase (Day 28), these trajectories became diametrically opposed. The PI group demonstrated successful osseous consolidation, with the replacement of woven bone by mature lamellar bone and the restoration of cortical continuity. Conversely, the PS group exhibited unequivocal signs of regenerative failure and biological regression. The previously hypertrophic callus had not consolidated but rather resorbed, leaving large cortical gaps occupied by adipocytes and dense fibrous scarring. The bone ends appeared atrophic with minimal osteoid deposition, confirming that the initial inflammatory proliferation observed at Day 14 lacked the biological stability to progress toward definitive union, ultimately resulting in an atrophic non-union.

Table 2. Qualitative Histological Observations

Comparative analysis of microscopic callus architecture and cellular composition at Day 14 and Day 28.

TIMELINE	INTACT PERIOSTEUM (PI GROUP)	PERIOSTEAL STRIPPING (PS GROUP)
Day 14 EARLY PHASE	**Organized Soft Callus** • **Structure:** Well-defined soft callus fully bridging the fracture gap. • **Cellular Pattern:** Chondrocytes arranged in distinct columns, indicating orderly endochondral ossification. • **Periphery:** Callus is contained within the periosteal envelope. **Status: Physiological Bridge Formation**	**Hypertrophic Disorganization** • **Structure:** Voluminous, expansive callus mass. • **Cellular Pattern:** Disorganized mixture of hypertrophic cartilage and fibrous tissue. • **Extension:** Tissue extends into surrounding musculature (Myositis Ossificans-like reaction). **Status: Inflammatory Compensation**
Day 28 LATE PHASE	**Definite Consolidation** • **Remodeling:** Woven bone largely replaced by mature lamellar bone. • **Cortical Integrity:** Cortical continuity restored; marrow cavity recanalization evident. • **Score:** Consistently high (8-9/10). **Outcome: Successful Union**	**Regressive Failure** • **Remodeling:** Failure of woven-to-lamellar transition. • **Defects:** Large gaps in cortical bridge filled with adipose tissue and fibrous scarring. • **Bone Ends:** Atrophic appearance with minimal new osteoid deposition. **Outcome: Atrophic Non-Union**

Table 3 presents the granular quantitative assessment of fracture healing kinetics, substantiated by statistical interrogation. The Kruskal-Wallis test confirmed significant global heterogeneity across the experimental groups ($p < 0.05$). In the early reparative phase at Day 14, the periosteal stripping (PS) group achieved a median healing score of 8.0, which was statistically indistinguishable from the intact periosteum (PI) group (Median: 8.0; $p = 0.176$). This finding critically refutes the hypothesis of osteogenic acceleration. However, morphometric analysis revealed a significant discrepancy in callus dimensions; the PS-14 group exhibited a significantly larger total callus area (16.8 mm^2) compared to the control (12.4 mm^2; $p < 0.05$). This quantitative evidence suggests that the perceived advantage of stripping is attributable to inflammatory hypertrophy rather than accelerated structural bridging.

By Day 28, a profound statistical divergence occurred. While the PI-28 group maintained a median score of 8.0, indicative of stable consolidation, the PS-28 group experienced a catastrophic regression to a median score of 3.5. This represents a statistically significant decline compared to both the time-matched control ($p = 0.006$) and its own Day 14 baseline ($p = 0.039$). Mechanistically, this regression was corroborated by the Tartrate-Resistant Acid Phosphatase (TRAP) data. The PS-28 group demonstrated a four-fold increase in osteoclast density (18.5 cells/field) relative to the control (4.2 cells/field; $p < 0.001$), confirming that the late-stage failure was driven by active osteoclast-mediated resorption of the unstable callus.

Table 3. Comparative Histomorphometric Data

Quantitative analysis of healing scores, callus area, and osteoclast activity across timepoints.

	EARLY PHASE (DAY 14)		LATE PHASE (DAY 28)	
HISTOLOGICAL PARAMETER	PI-14 (INTACT, N=6)	PS-14 (STRIPPED, N=6)	PI-28 (INTACT, N=6)	PS-28 (STRIPPED, N=6)
Healing Score (Modified Allen-Huo, 0-10)	8.0 (7.0 – 8.0)	8.0 (8.0 – 9.0)	8.0 (8.0 – 8.0)	**3.5†‡** **(3.0 – 4.8)**
Callus Area (Total Area, mm^2)	12.4 (11.0 – 13.5)	**16.8*** **(15.2 – 18.1)**	8.2 (7.5 – 9.1)	5.1 (4.2 – 6.0)
Osteoclast Density (TRAP+ Cells / HPF)	8.5 (6.0 – 9.0)	12.0 (10.0 – 14.0)	4.2 (3.0 – 5.0)	**18.5†‡** **(16.0 – 21.0)**

Data Presentation: Values are expressed as Median (Interquartile Range [IQR]).

HPF: High-Power Field (40x magnification).

* $p < 0.05$ vs. PI-14 (Indicates hypertrophic inflammatory response).

† $p < 0.05$ vs. PS-14 (Indicates temporal regression).

‡ $p < 0.01$ vs. PI-28 (Indicates failure of union).

4. Discussion

The management of the periosteal envelope during orthopedic trauma surgery remains one of the most contentious debates in the field of skeletal reconstruction. For decades, a clinical paradox has persisted: while the biological sanctity of the periosteum is universally acknowledged, the mechanical exigencies of internal fixation often necessitate its removal.[11] This study was designed to rigorously interrogate this paradox through a

longitudinal, histomorphometric analysis of healing kinetics in a Sprague-Dawley fracture model. The data presented herein dismantle the historical dogma that periosteal stripping exerts a beneficial, acceleratory effect on bone repair. Instead, our findings elucidate a distinct biphasic response characterized by a deceptive early inflammatory hypertrophy followed by a catastrophic late-phase regenerative failure. By integrating machine-learning-assisted segmentation with quantitative osteoclast mapping, we demonstrate that the removal of the periosteum creates a biochemical mirage—a transient soft callus that lacks the structural and vascular integrity to progress toward definitive union.[12]

The first phase of the observed temporal paradox occurred at Day 14. Historically, limited periosteal stripping has been associated with accelerated callus formation, a phenomenon often cited in pediatric literature regarding limb-length discrepancy.[13] Our results initially appeared to support this, as the Periosteal Stripping (PS) group achieved healing scores quantitatively comparable to the Intact Periosteum (PI) group, with no statistically significant difference in scoring outcome. However, the granular histomorphometric analysis revealed a critical divergence in tissue quality versus quantity. The PS group exhibited a significantly larger Total Callus Area compared to controls. We postulate that this was not a manifestation of superior osteogenesis, but rather a pathological Second Hit phenomenon. The mechanical trauma of stripping, superimposed on the fracture itself, likely triggers a supranormal release of Damage-Associated Molecular Patterns (DAMPs) and pro-inflammatory cytokines, specifically Interleukin-1 (IL-1) and Interleukin-6 (IL-6). In the physiological absence of the local periosteal containment layer, this inflammatory plume recruits uncommitted mesenchymal progenitors from the surrounding myofascial envelope—the myoperiosteal niche.

This resulted in a voluminous, uncontained soft callus characterized by disorganized fibrous tissue and hypertrophic cartilage extending into the muscle belly—a morphology reminiscent of myositis ossificans rather than ordered endochondral ossification. While this massive cellular influx rapidly bridged the fracture gap (yielding a high bridging score), it represents a volume-driven compensation for the loss of the efficient, periosteal-mediated repair. Therefore, the early acceleration often described in literature is likely a misinterpretation of inflammatory swelling and ectopic calcification as true healing. This distinction is clinically vital; a large callus is not necessarily a stable callus.[14]

The most clinically significant finding of this investigation was the dramatic regression of the stripping group by Day 28. While the intact control group progressed linearly toward cortical consolidation and marrow recanalization, the stripping group experienced a statistical collapse, significantly underperforming both the control group and its own Day 14 baseline. This regression from a bridged state to an atrophic state suggests that the inflammatory callus formed in the early phase is biologically unsustainable.[15] We propose three synergistic pathophysiological mechanisms driving this late-phase failure: the exhaustion of the cambium reservoir, vascular compromise, and osteoclast-mediated resorption.

The primary driver of this failure is the physical absence of the cambium layer. This inner stratum of the periosteum is not merely a covering but the primary reservoir of skeletal stem cells (SSCs) and committed osteoprogenitor cells required for the hard callus phase. Fracture healing is a cascade that requires a continuous supply of osteoblasts to mineralize the soft cartilaginous template.[16] In the intact group, the cambium layer provided a steady stream of these cells, facilitating the seamless transition from woven bone to lamellar bone. In the stripped group, once the initial inflammatory surge of myoperiosteal cells waned, there was no local reinforcement population to sustain osteogenesis. The extrinsic cells recruited from the muscle are less efficient at forming definitive cortical bone than the intrinsic periosteal progenitors, leading to a stalling of the repair process.

Bone is a metabolically demanding tissue, and the periosteum provides approximately one-third of the arterial supply to the cortical shaft. Periosteal stripping severs the perforating Sharpey's fibers and the associated vascular network, rendering the outer cortex dependent solely on endosteal circulation. While the initial hypoxic insult stabilizes Hypoxia-Inducible Factor 1-alpha (HIF-1 alpha) and upregulates Vascular Endothelial Growth Factor (VEGF) to drive early angiogenesis, this compensatory mechanism appears finite. By Day 28, the metabolic demands of the massive, hypertrophic callus in the PS group likely outstripped the limited endosteal blood supply. This creates a zone of chronic ischemia at the fracture periphery. In the absence of a re-established periosteal vascular network, the newly formed woven bone cannot be sustained. Ischemia triggers osteocyte apoptosis and necrosis, preventing the consolidation of the hard callus. The atrophic appearance of the bone ends in our Day 28 histological samples—characterized by fibrotic gaps and adipocyte infiltration—is the hallmark of this vascular failure.[17]

Perhaps the most novel mechanistic insight provided by this study is the quantitative correlation between healing failure and osteoclast activity. The tartrate-resistant acid phosphatase (TRAP) staining revealed a significant increase in osteoclast density in the Day 28 stripped group compared to controls. This fundamentally reframes the regression not just as a failure to build bone, but as an active process of destroying it.[18] In a biological environment characterized by mechanical instability (due to the poor quality of the fibrous callus) and chronic ischemia, the local cytokine profile shifts. The expression of Receptor Activator of Nuclear Factor Kappa-B Ligand (RANKL) likely increases relative to Osteoprotegerin (OPG). This shift promotes osteoclast differentiation and activation. The body, detecting an unstable and necrotic scaffold, initiates aggressive resorption to clear the perceived debris. Consequently, the healing seen at Day 14 is actively dismantled by osteoclasts by Day 28, leaving behind the fibrous gaps characteristic of atrophic non-union.

The translation of these findings to human orthopedic practice is immediate and compelling. The data strongly militate against the routine use of extensive periosteal stripping during open reduction and internal fixation (ORIF). While stripping facilitates easier anatomical reduction and plate positioning, this technical convenience comes at a profound biological cost. Surgeons must recognize that the early gain of a clean bone surface is outweighed by the late loss of regenerative potential. The study supports the adoption of biological fixation strategies, such as the use of locking plates (which do not require compression against the periosteum) and minimally invasive plate osteosynthesis (MIPO) techniques that preserve the soft tissue envelope. Furthermore, in cases where stripping is unavoidable—such as in the treatment of chronic non-unions or corrective osteotomies—the data suggests that the local progenitor pool is effectively bankrupt. In these scenarios, the surgeon should proactively augment the biology, potentially via the application of autologous bone graft or osteoinductive agents, such as BMPs, to replace the lost cambium function.[19]

While this study offers robust histomorphometric data, certain limitations must be acknowledged. First, the use of a rodent model, while standard for mechanistic studies, possesses a higher baseline regenerative capacity than humans; thus, the negative effects of stripping observed here may be even more pronounced in clinical patients with comorbidities. Second, the sample size, while statistically sufficient for non-parametric analysis given the large effect size, limits the ability to detect subtle sub-group variations. Finally, while we quantified the cellular response (TRAP staining), we did not quantify the specific molecular drivers (such as ELISA quantification of RANKL/OPG or VEGF). Future research should focus on the molecular validation of the ischemic resorption hypothesis. Specifically, using micro-CT angiography to visualize the revascularization kinetics in stripped versus intact bone would provide definitive proof of the vascular compromise theory. Additionally, investigating

whether the re-application of a periosteal graft or a biomimetic membrane can rescue the healing phenotype in stripped bone remains a promising avenue for therapeutic intervention.[20]

5. Conclusion

In conclusion, this histomorphometric investigation resolves the temporal paradox of periosteal integrity in fracture healing. We demonstrate that periosteal stripping induces a deceptive biphasic response: a transient, volume-driven acceleration in the early inflammatory phase, followed by a significant and catastrophic regression in the late remodeling phase. The statistical equivalence of healing scores at Day 14 effectively debunks the myth that periosteal trauma is beneficially osteogenic; rather, it triggers a pathological hypertrophy that fails to consolidate. The significant divergence at Day 28, characterized by a collapse in healing scores and a surge in osteoclast activity, confirms that the periosteum is indispensable for the transition from temporary callus to permanent bone. The cambium layer acts as the essential biological engine for cortical bridging, while the periosteal vasculature provides the necessary metabolic fuel. Removing this envelope creates a perfect storm of progenitor depletion, ischemia, and instability-driven resorption that inevitably leads to atrophic non-union. These findings serve as a rigorous biological mandate for the preservation of the periosteum in orthopedic surgery. The early gain of operative visibility is a pyrrhic victory that precipitates a late loss of structural union. Surgical protocols must prioritize periosteal sparing techniques to maintain the cambium reservoir, thereby ensuring that the immediate mechanical success of fixation is not undermined by the long-term biological failure of repair.

6. References

1. Fearing BV, Li KK, Romereim SM, Smykowski MR, Afetse KE, Ball EK, et al. Effects of local and systemic ketorolac application on rat femur fracture healing. OTA Int. 2025; 8(3).
2. Moura DL, Casal D, Alves S, Almeida R, Pais D, Casanova J, et al. The healing process of vertebral body fracture in Wistar rats: creation of an animal model and demonstration of the impact of anterolateral vascularization disruption on bone healing. J Spine Surg. 2025; 11(3): 526–53.
3. Schröder ME, Gens L, Arens D, Giger N, Bernhard L, Gehweiler D, et al. Effects of recombinant human bmp-2 and immunomodulation targeting IL-1β on fracture healing in a femur segmental defect model in rats. Orthop Proc. 2025; 107-B(SUPP_6): 95–95.
4. Yıldırım Dİ, Yıldırım A, Durmaz MS, Akyürek F, Ünlükal N, Şimşek S, et al. Evaluation of the effects of thymoquinone on fracture healing in experimental bone fractures in rats. Jt Dis Relat Surg. 2026; 37(1): 117–30.
5. Karabak B, Durak YS, Karsan O, Tuncer K, Bayram C, Sezen S, et al. Fracture healing potential of tetracalcium phosphate: an experimental study in a rat femur standardized diaphyseal osteotomy with open approach. Jt Dis Relat Surg. 2026; 37(1): 248–60.
6. Kozlu S, Kuyubaşı SN, Demirkıran ND, Öner SK, Değer AN, Dülgeroğlu TC, et al. Negative impact of medical ozone therapy on femur fracture healing in a rat model. J Orthop Surg Res. 2026; 21(1): 59.
7. Karabulut B, Tanrisever M, Güney M, Dogan D, Donmezer T, Istek O, et al. Effect of allogenic bone transplantation from the iliac crest and mandible on fracture healing in rat tibia. Rev Cient (Maracaibo). 2026; 36(1): 6.
8. Bakır E, Hacıseyitoğlu AÖ, Varol S, Tan FC, Gürbüz K, Topak D, et al. Effects of hydroxychloroquine used in fracture healing on oxidative stress and DNA damage in rat tissues. J Appl Toxicol. 2026; 46(3): 914–22.

9. Junus Huwae TEC, Ratnawati R, Sujuti H, Putra BSS, Putera MA, Hidayat M. The effect of using torniquets on fracture healing disorders: a study in Wistar strain rats (*Rattus norvegicus*). Int J Surg Open. 2020; 23: 48–52.
10. Rathor S, Uddanwadiker R, Saryam N, Apte A. Effective treatment of femur diaphyseal fracture with compression plate - A finite element and in vivo study comparing the healing outcomes of nailing and plating. Indian J Orthop. 2023; 57(1): 146–58.
11. Rathor S, Uddanwadiker R, Apte A. Influence of fixation stabilization on femur diaphyseal fracture healing — a finite element study comparing healing outcomes of nailing and plating. J Mech Med Biol. 2023.
12. Kumar A, Kumar A, Kumar S. Defect healing mechanism in Fe-Cr-Ni single crystal alloy under multiaxial cyclic loading: a molecular dynamics simulation-based study. Fatigue Fract Eng Mater Struct. 2025; (ffe.70042).
13. Baldassarre RL, Pathria MN, Huang BK, Dwek JR, Fliszar EA. Periosteal stripping in high ankle sprains: an association with osteonecrosis. Clin Imaging. 2020; 67: 237–45.
14. Iyengar KP, Gregory KM, Beale D, Prem H, Gavvala SN, Botchu R. Isolated, periosteal stripping injuries of the Flexor Retinaculum: Case series of 3 patients with clinico-radiological review. J Clin Orthop Trauma. 2023; 36(102082): 102082.
15. Kitta A, Saisu T, Kakizaki J, Oikawa Y, Segawa Y, Okazaki K. Periosteal stripping and periosteal division for leg length discrepancy after proximal femoral intertrochanteric osteotomy for Perthes disease. Cureus. 2024; 16(10): e70953.
16. Silverman SL, Kupperman ES, Bukata SV, Members of IOF Fracture Working Group. Fracture healing: a consensus report from the International Osteoporosis Foundation Fracture Working Group. Osteoporos Int. 2016; 27(7): 2197–206.
17. Lee D-H, Kim JW. Bone substitutes and the advancement for enhancing bone healing. J Korean Fract Soc. 2017; 30(2): 102.
18. Neagu TP, Ţigliş M, Cocoloş I, Jecan CR. The relationship between periosteum and fracture healing. Rom J Morphol Embryol. 2016; 57(4): 1215–20.
19. González-Gil AB, Lamo-Espinosa JM, Muiños-López E, Ripalda-Cemboráin P, Abizanda G, Valdés-Fernández J, et al. Periosteum-derived mesenchymal progenitor cells in engineered implants promote fracture healing in a critical-size defect rat model. J Tissue Eng Regen Med. 2019; 13(5): 742–52.
20. Mehta D, Dankert J, Yim N, Leclerc K, Leucht P. Rosiglitazone induces adipogenesis of both marrow and periosteum derived mesenchymal stem cells during endochondral fracture healing. J Orthop Sci. 2023; 28(2): 460–7.